Quantum Electronics **51** (3) 222–227 (2021) ©2021 Kvantovaya Elektronika and IOP Publishing Limited

INTERACTION OF LASER RADIATION WITH MATTER. LASER PLASMA https://doi.org/10.1070/QEL17443

Capture of a dipolar magnetic field by laser-produced plasma

M.A. Efimov, A.A. Chibranov, A.G. Berezutsky, M.S. Rumenskikh, V.G. Posukh, Yu.P. Zakharov, E.L. Boyarintsev, P.A. Trushin, E.V. Smolina, I.B. Miroshnichenko, I.F. Shaikhislamov

Abstract. **We describe an experiment on the interaction of a dipolar magnetic field with the laser plasma flow produced inside of a laboratory magnetosphere. This interaction is found to exhibit two dynamic stages: after a prompt displacement of the dipole field by the laser plasma, the magnetic field is captured and carried outside of the magnetosphere. The resultant data confirm the results of previous measurements carried out far beyond the magnetosphere and provide additional information about the new process of capturing the dipolar magnetic field by the internal magnetospheric plasma flow.**

Keywords: *laser-produced plasma, magnetic field, magnetosphere.*

1. Introduction

Despite the rapid development of methods for numerical simulation of cosmic plasmas, laboratory experiments and experimental confirmation of their models are still the basis for studying plasma physics. One of the areas in which the results of laboratory experiments were used to construct theories and numerical models is the interaction of counterpropagating plasma flows in the presence of a magnetic field. The 1970s–1980s saw the execution of several experiments with laser-produced plasmas expanding into a magnetised background plasma at a super-Alfven velocity [1–4] with the purpose of modelling artificial chemical ejections into the terrestrial magnetosphere. Proceeding from the resultant data, a new dynamic interaction model was developed: the magnetic laminar mechanism [5] or the interaction in the finite-Larmor-radius mode [6]. This model complemented the earlier kinematic model of electron substitution [7, 8]. Our recent experiments [9, 10] provided comprehensive data bearing out both models.

The study of the magnetosphere is also one of the areas in which laboratory modelling has been extensively used. The theoretical basis was laid in Refs [11–13], and a review of experimental works is given in Ref. [14]. This research was carried out on the KI-1 facility using two pulsed plasma generators: an induction Θ-pinch plasma and the plasma generated by a CO_2 laser, whose plasma fluxes interact with compact magnetic dipoles [15, 16]. The combination of these two plasma sources, whose plasmas have very different energy and spatio-temporal characteristics, made it possible to model ejections in the circumterrestrial space and the effects of solar plasma ejections [17–19]. The longitudinal currents connecting the boundary layer of the magnetosphere with the polar ionosphere were studied on the basis of model experiments [20, 21]. Also modelled was the pulse of solar wind plasma with a frozen-in transverse magnetic field interacting with the magnetosphere [22]. The flow with the transverse frozen-in field was produced in the expansion of the laser plasma across the magnetic field into the background plasma, which filled the vacuum chamber along the lines of the external magnetic field prior to interaction. The object like a mini-magnetosphere, which can potentially exist around magnetised asteroids and which was discovered above lunar magnetic anomalies [23], is also studied on the KI-1 facility. It was laboratory experiments that provided the necessary data for the formulation and verification of the Hall model [24–26], which explains the unusual features of the mini-magnetosphere observed in earlier numerical simulations [27, 28]. Recorded in one of the latest laboratory experiments were the fluxes of magnetically reflected ions, which were qualitatively similar to those observed above lunar magnetic anomalies [29].

A fundamentally new combination of interacting fluxes and a magnetic field was investigated in the experiment of Ref. [30]. The Θ-pinch plasma filled the vacuum chamber and produced a magnetosphere with an estimated size of about 30 cm around the magnetic dipole. The special feature was that the laser plasma was generated inside this magnetosphere at two targets symmetrically located on the dipole body (Fig. 1). The laser-produced plasma moved in opposition to the Θ-pinch plasma flow and had enough kinetic energy to force out the dipole magnetic field. Executing this experiment was motivated by the discovery of new astrophysical objects – hot Jupiters orbiting extremely close to the star and experiencing a supersonic outflow of the upper atmosphere [25]. The interaction of the expanding planetary flow with the planetary magnetic field results in a variety of previously unexplored phenomena [31, 32]. The main energy parameter of the problem is the position of the Alfven point (the distance at which the energy density of the plasma flow becomes equal to the energy density of the magnetic field), measured in units of the planet radius, R_A/R_P. The experimental modelling of plasma outflow in a dipole field was first carried out in Ref. [33] with

M.A. Efimov, A.A. Chibranov, A.G. Berezutsky, M.S. Rumenskikh, V.G. Posukh, Yu.P. Zakharov, E.L. Boyarintsev, P.A. Trushin, E.V. Smolina, I.B. Miroshnichenko, I.F. Shaikhislamov Institute of Laser Physics, Siberian Branch, Russian Academy of Sciences, prosp. Akad. Lavrent'eva 15B, 630090 Novosibirsk, Russia; e-mail: mikle3496@gmail.com

Received 17 September 2020; revision received 2 December 2020
Kvantovaya Elektronika **51** (3) 222–227 (2021)
Translated by E.N. Ragozin

the use of an annular pulsed discharge. Realised in this case was the ratio $R_A/R_P \approx 3$, which corresponds to the hot Jupiters with a rather high magnetic field. In Ref. [30], the planetary flow was modelled by laser-produced plasma and the conditions of a relatively weak magnetic field, $R_A/R_P \approx 1$, were realised.

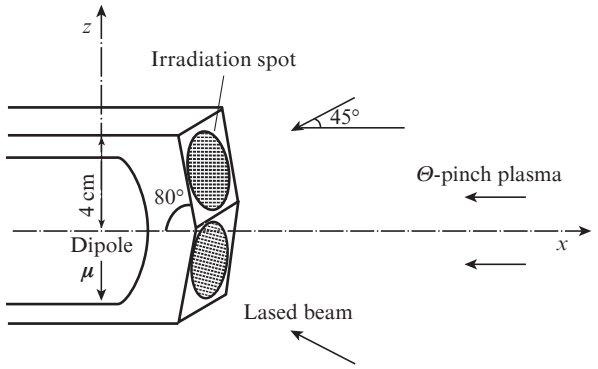

Figure 1. Schematic of laser irradiation of the target located on the dipole body.

In Ref. [30], the probe measurements were carried out far beyond the magnetosphere, and it was found that the laser-produced plasma, which passes through the background plasma, partially displaces it due to Coulomb collisions and carries magnetic field with it, which is an order of magnitude stronger than that of the vacuum dipole field at these distances. The resultant data testify to a new and unexpected effect of the capture of the magnetospheric field by laser-produced plasma and its subsequent 'entrainment' over long distances. Note that in all previous experiments with relatively simple magnetic field geometry the laser plasma manifested itself as a good diamagnet. Due to the relatively high expansion rate, high density and temperature at the initial stage of expansion, the magnetic field is efficiently forced out from the volume occupied by the laser plasma. Comparing the results of Refs [33] and [30] suggests that the detected effect can be reproduced using only laser-produced plasma.

To obtain more information about the detected effect, detailed measurements inside the magnetosphere were carried out in the present experiment. The results of our measurements confirm the effect of magnetospheric field capture by laser-produced plasma and demonstrate new details of how this occurs. In particular, it is found that the expected phase of almost complete forcing-out of the dipole field does exist at the front of the laser-produced plasma, which is quickly replaced by the phase of magnetic field capture.

2. Experimental conditions and results

Our experiments were carried out on the KI-1 facility, which comprises a 500-cm long chamber 120 cm in diameter operating at a residual pressure of 10^{-6} Torr (Fig. 2). An induction Θ-pinch with an output aperture 20 cm in diameter ejects for $\sim$100 μs a completely ionised hydrogen plasma, which propagates along the chamber axis. In the typical Θ-pinch operating mode, the average background plasma density was $(5\pm2)\times10^{12}$ cm^{-3} and the plasma velocity was 45 ± 15 km s^{-1}. To stabilise the background plasma flow along the chamber axis, a weak magnetic field (5 Gs) was generated, which did not introduce any noticeable effects into the plasma interactions under study. The magnetic dipole was located at a distance of 290 cm from the output aperture of the Θ-pinch. The magnetic moment, which was $\mu = 1.1\times10^6$ Gs cm^3, was perpendicular to the chamber axis. The time of maintaining the dipole magnetic field was 250 μs. The dipole had the shape of a cylinder with a diameter and height of 5 cm with an epoxy coating, on which a polyethylene target was fixed. Two beams of CO_2-laser radiation with a pulse duration of 70 ns and an energy of 150 J each were symmetrically focused through a system of lenses and mirrors to spots approximately 2 cm in size (Fig. 1). The arrangement of the targets on the dipole body and their irradiation are schematised in Fig. 2. The laser plasma was generated approximately 30 ± 5 μs after the onset of background plasma production. The use of a laser to produce an internal magnetospheric plasma flow that expands outward and pulls out the magnetic field lines has fundamental advantages. In the first attempts to 'inflate' the dipole magnetic field, use was made of an electric electrode discharge in a gas jet [34]. In Ref. [33], the plasma was produced by a discharge along the surface of a cable wound on the dipole body. In both cases, the energy density was relatively low, and the discharge plasma carried strong parasitic electric and magnetic fields and currents due to the presence of electrodes in the interaction region. The effect described below cannot be achieved without the use of laser-produced plasma.

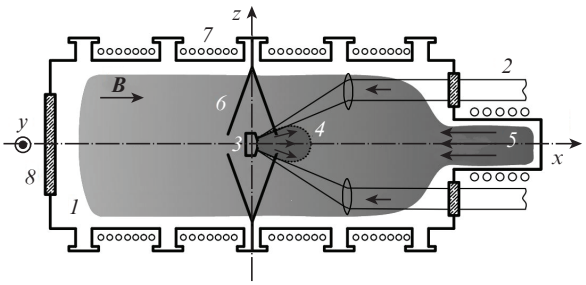

Figure 2. Schematic of the experiment:
(*1*) vacuum chamber; (*2*) CO_2-laser radiation; (*3*) dipole with the target attached to it; (*4*) laser-produced plasma flow; (*5*) background plasma flow; (*6*) magnetic and electric probes; (*7*) coils inducing external magnetic field along the vacuum chamber; (*8*) viewing window; (***B***) magnetic field.

The means of diagnostics comprised combined Langmuir and three-component magnetic probes, as well as an ion collector. The main measurements were carried out along the axis of interaction with the movement of the probes from the dipole through the magnetosphere and further into the background plasma flow. To present the results, the so-called geomagnetic coordinate system is used, as shown in Fig. 1. Its x axis is directed in opposition to the background plasma flow (an analogue to the solar wind), and the z axis is directed oppositely to the magnetic moment of the dipole. Figure 3 shows typical waveforms of the ion current density measured by the Langmuir probe and collectors placed at different distances from the dipole. Figure 3a shows the results obtained in the presence of only the background plasma (no laser-produced plasma, dipole off), which demonstrate the temporal dynamics of the flow and allow us to calculate its velocity. Note that the background plasma source (Θ-pinch) is located

at a distance $x = 290$ cm, and so the further the probe is removed from the dipole, the closer it is to the Θ-pinch. Figure 3b shows the results obtained in the presence of laser-produced plasma and with the dipole switched on. The slit of the collector placed at a distance $x = 70$ cm was rotated by 180°, so that it recorded the laser-produced plasma, but did not see the background one. The collector at $x = 15$ cm was still oriented to the background plasma, but was displaced along the y axis to a point with the coordinate $y = 17$ cm to be outside of the magnetosphere. Up to the zero point in time, at which the laser produces the plasma on the target, the probes at the points $x = 140$ and 15 cm record the background plasma flow, approximately the same as in the previous case. After target irradiation at the point in time $t = 0$, the collector at the point $x = 70$ cm demonstrates the dynamics of the laser-produced plasma. In this case, the collector at the point $x = 15$ cm shows a sharp decrease in the background plasma flow, which is due to its 'sweeping out' by the counterpropagating laser-produced plasma flow.

The typical parameters of the background plasma near the dipole were as follows: the duration of the flow ~20 μs, its velocity ~100 km s^{-1}, and density $\sim 5 \times 10^{12}$ cm^{-3}. At a distance $x = 70$ cm the velocity of laser-produced plasma front is ~250 km s^{-1} and the plasma density is $\sim 2 \times 10^{12}$ cm^{-3}. According to previous measurements [30], the laser plasma flow consists by half of protons and by half of carbon ions C^{2+}, C^{3+}, C^{4+}.

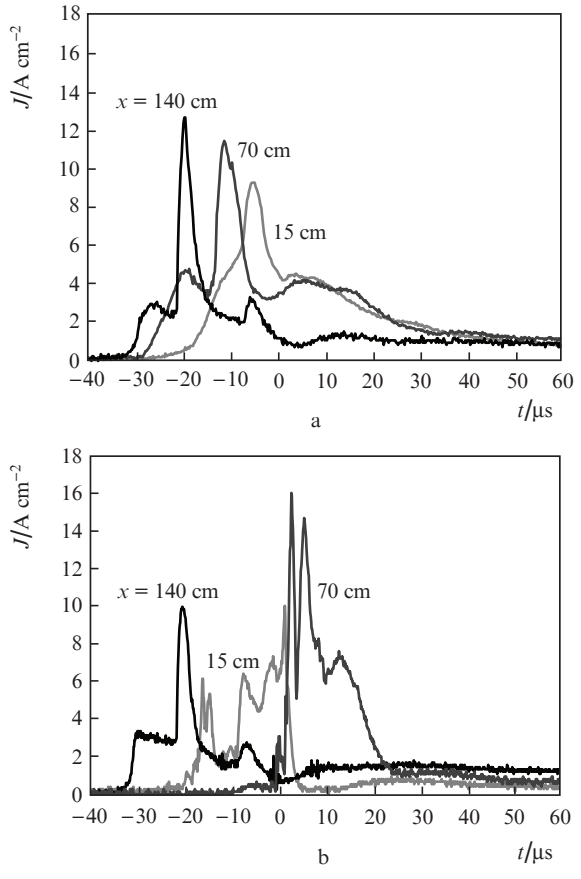

Figure 3. Typical waveforms of the ion density current J in the plasma measured with the Langmuir probe at a distance $x = 140$ cm as well as with collectors at distances $x = 70$ and 15 cm (a, b). In Fig. 3b, the collector at the point $x = 15$ cm is shifted along the y axis to the point $y = 17$ cm, and the collector at the point $x = 70$ cm is rotated by 180° towards the laser target.

The main results are presented in Fig. 4 in the form of perturbation waveforms of the three components of the magnetic field, ion density, and plasma potential at four distances from the dipole inside and at the boundary of the magnetosphere. The laser-produced plasma flow in the region under consideration has a clearly defined leading edge, which travels at a velocity of ~250 km s^{-1}, and a trailing edge (velocity: ~150 km s^{-1}) with a total duration of 4 to 6 microseconds, which corresponds to the length of the bunch of ~100 cm. The laser produces the plasma at two targets, and the flows add up on the x axis. Since the angular velocity distribution relative to the normal is proportional to $\cos\theta$ for each target, the total density on the axis has a complex distribution and decreases much more slowly than the inverse-cubed distance, as is observed in the case of a single target.

The plasma potential at short distances from the target ($x = 9$ and 13 cm) is positive prior to the arrival of the laser-produced plasma (i.e., during the flow of the background plasma around the dipole) and negative after its arrival. The positive floating potential is caused by background plasma ions penetrating in small amounts into the magnetosphere, and the highest potential reflects the highest energy of the oncoming flow ions (~100 eV). In a dense plasma, the potential is induced by electrons and is reflective of their temperature. One can see from Fig. 4 that the potential is negative at a distance $x = 26$ cm prior to the arrival of the laser-produced plasma, which indicates the presence of the flow of the background plasma at this point. Namely, the density calculated from the measured current density is $\sim 6 \times 10^{12}$ cm^{-3} prior to the arrival of the laser-produced plasma, while at shorter distances the Langmuir probe signal from the background plasma is absent, because it does not penetrate into the magnetosphere (except for a small number of ions). At a distance $x = 18$ cm, the potential is close to zero prior to the arrival of the laser-produced plasma. These data therefore suggest that the background plasma flow produces a magnetosphere of size $R_m \approx 20$ cm. The background-plasma temperature is estimated at ~10 eV and that of the laser-produced plasma at ~50 eV.

We consider the perturbation of the main magnetic component δB_z. On the axis, the dipole field has only a positive component, equal at the corresponding points to about 1500 Gs ($x = 9$ cm), 470 Gs ($x = 13$ cm), 190 Gs ($x = 18$ cm), 60 Gs ($x = 23$ cm). At all four distances, the recorded perturbation has a negative phase at first, which is quickly replaced by a positive one. A negative signal corresponds to the forcing-out of the existing field. It is precisely the forcing-out of the external magnetic field that is the well-known result of its interaction with laser-produced plasma, which was observed in previous experiments for a simpler magnetic field geometry. Note that the greatest value of the negative signal corresponds well to the total forcing-out of the initial field at distances of 13 and 18 cm. At a distance of 9 cm, the forcing-out is not complete, but rather significant. At a distance of 26 cm, the negative phase of the perturbation is absent during the passage of the laser-produced plasma, and there is only the forcing-out of the field by the background plasma. Forcing out the dipole field by the background plasma is an additional indication that the magnetosphere under production has a size of less than 26 cm.

One can see that the forcing-out phase at the front of laser-produced plasma lasts for only a short time (<1 μs). A

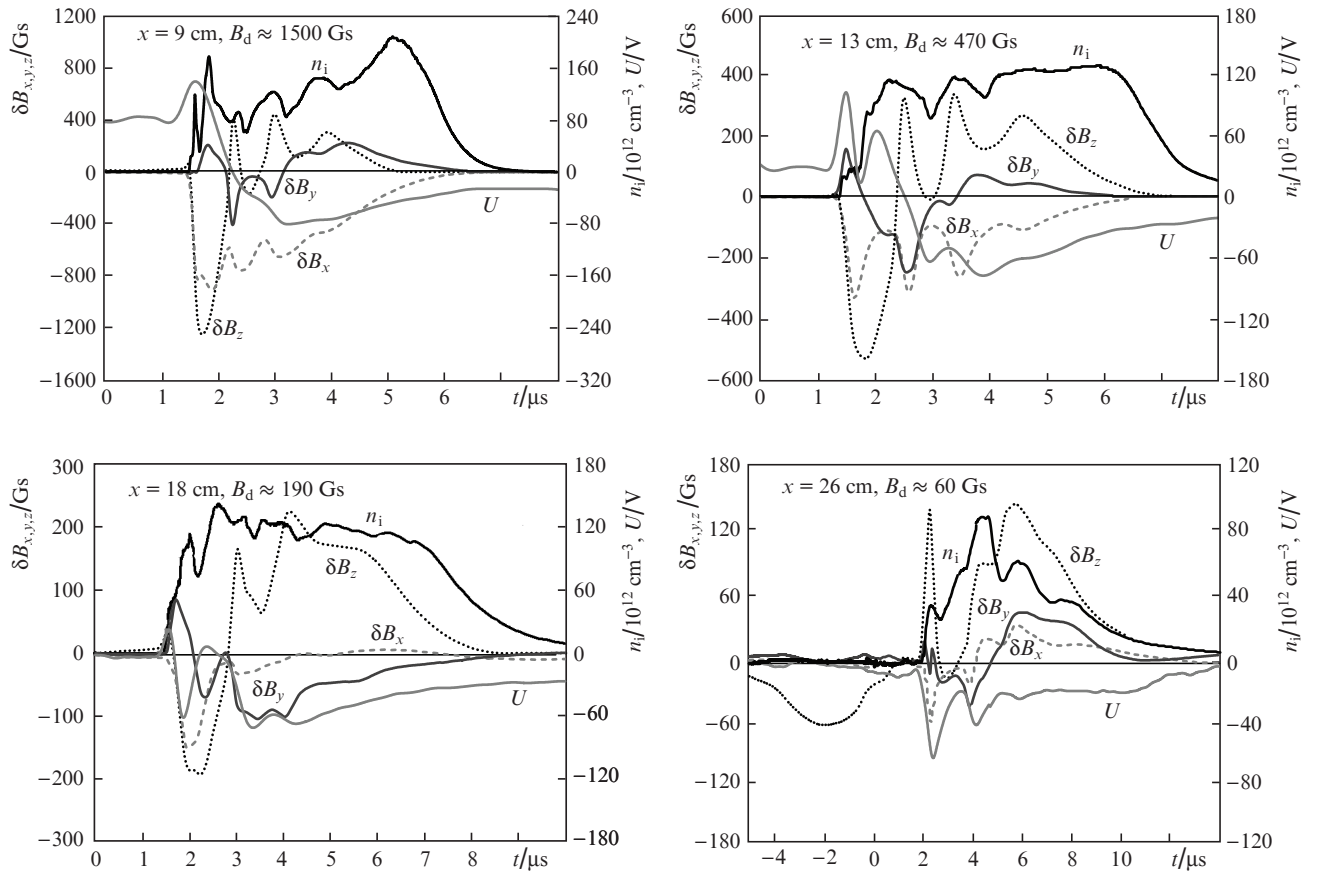

Figure 4. Waveforms of the magnetic field components δB_z, δB_x and δB_y, density n_i, and potential U at different distances along the x axis at which measurements were made and at different dipolar magnetic fields $\boldsymbol{B}_d$.

new fact observed in the present experiment is a prompt occurrence of the positive field perturbation phase, which testifies to an enhancement of the external magnetic field. The change of polarity is clearly seen at distances of 9, 13, and 18 cm, i.e. inside the magnetosphere. It is clearly seen that the positive phase has pronounced maxima that coincide with the local maxima of the laser-produced plasma flow. At a distance of 26 cm, the negative phase associated with the laser-produced plasma is absent. Instead, a positive phase already occurs with the arrival of the laser-produced plasma front, i.e. the field enhancement. This is supposedly due to the fact that this point is located outside the magnetosphere. The amplitude of the field in the positive phase of its enhancement decreases with distance and is approximately 300, 200, 150 and 100 Gs for $x = 9$, 13, 18 and 26 cm, respectively. The dependence is quite close to the dependence of the form $\delta B_z \propto 1/x$.

Since the laser-produced plasma flows are not perfectly symmetric with respect to the xy plane, other components are also observed in addition to the main δB_z component. The perturbation of the second dipole component δB_x does not show the change of polarity of the signal and the forcing-out phase of the field. Figure 5 shows the signal waveforms measured above the equator at an angle $\varphi \approx 45°$ for a radial distance $R \approx 14$ cm from the dipole centre. One can see that the laser-produced plasma flux, as well as the temperature, is an order of magnitude lower at this angle than in the equatorial plane (Fig. 4), which corresponds to a relatively small solid angle of expansion of the plasma plume. The perturbation of the magnetic field is also relatively small. However, the forcing-out phase of the δB_x component is clearly observed, which is succeeded by the enhancement phase. The δB_z component also shows field enhancement. Therefore, the geometry of the perturbation of the magnetic field lines indicates the inflation of the dipole magnetic field and the stretching of the field lines.

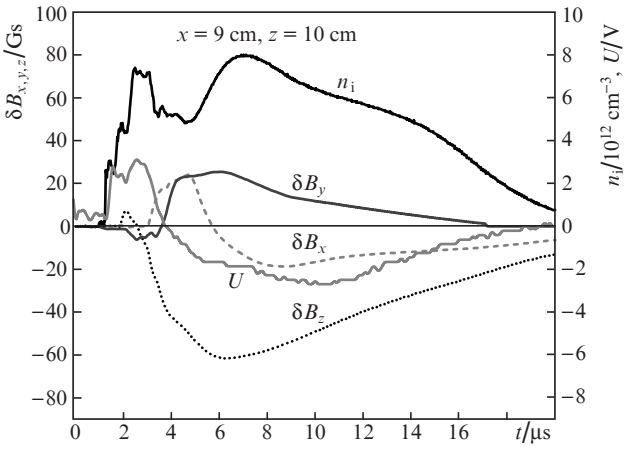

Figure 5. Waveforms of the magnetic field components δB_z, δB_x and δB_y, the density n_i, and the potential U measured above the equatorial plane.

3. Conclusions and discussion of resultant data

Given below are the most important dimensional and dimensionless parameters of the Θ-pinch plasma, of the mini-magnetosphere produced about the magnetic dipole, and the laser-produced plasma, which forms inside the magnetosphere and expands into the background plasma (where C_s is the sound velocity, λ_{ii} is the mean free ion path, ω_{pi} is the ion plasma frequency, R_L is the Larmor radius, ω_e is the electron frequency, and τ_{ei} is the electron-ion collision frequency).

Background plasma parameters

Velocity V_*/km s^{-1}	100
Average density n/cm^{-3}	5×10^{12}
Mach number V_*/C_s	~3

Magnetosphere parameters

Magnetosphere dimension R_m/cm	~20
Relative dipole radius R_d/R_m	0.25
Knudsen number λ_{ii}/R_m	~20
Reynolds number $4\pi\sigma R_m V_*/c^2$	~1000
Hall parameter $R_m \omega_{pi}/c$	2.5
Ion magnetisation degree R_m/R_L	2

Parameters of laser-produced plasma

The ratio of the laser plasma energy to the magnetic energy of the dipole Q_{LP}/Q_d	~1
Velocity relative to the background V_{LP}/V_*	~2.5
Knudsen number λ_{ii}/R_m	~100
Reynolds number $4\pi\sigma R_m V_{LP}/c^2$	>1000
Electron magnetisation degree $\omega_e \tau_{ei}$	>100

The resultant mini-magnetosphere is sufficiently collisionless, and it is transitional in terms of the Hall parameter and magnetisation degree. The mini-microsphere properties for the indicated parameters were comprehensively studied in our previous work [25].

By and large the conditions differ slightly from the conditions of a similar experiment [30], in which the effect of capturing the magnetic field of a dipole by a laser-produced plasma was discovered. The purpose of the present experiment was to obtain additional data about this process. One can see that the waveforms immediately outside the magnetosphere (Fig.4, x = 26 cm) qualitatively correspond to the previously obtained results. A perturbation of the field is observed, which dynamically correlates with the laser plasma flow, which testifies to its transfer by the plasma. In this case, the perturbation has the same sign (direction) as the dipole field but far exceeds it in magnitude (δB_z = 100–150 Gs, $B_d \approx$ 60 Gs). Clearly traced inside the magnetosphere is the dynamic transition from the phase of forcing out the dipole field to the phase of its capture. The displacement phase is short and is observed only at the front of the laser-produced plasma stream.

Another feature, which was also observed in the previous experiment at long distances from the dipole, is the pronounced modulation of the captured magnetic field. The flow of laser-produced plasma consists of separate merged bunches. As discussed in our paper [20], the CO_2 laser radiation pulse has several peaks spaced at about 0.5 microseconds and produces at least three consecutive streams of laser-produced plasma that follow each other. The velocity of the first flow is 1.5–2 times higher than the velocity of the second one and 2–3 times higher than that of the third. Since two laser plumes add up on the x axis, the flow modulation has a greater number of maxima and minima. The modulation depth of the magnetic field is much greater than the modulation depth of the plasma density and is approximately 100%, i.e. the minimum value of the field lowers to almost zero.

The capture of the magnetic field may be interpreted as the field penetration into the electron liquid of laser-produced plasma. The problem is that the electron temperature and the plasma conductivity are rather high. The magnetic Reynolds number of the laser-produced plasma is greater than 10^3, and the magnetisation parameter $\omega_e \tau_{ei}$ is no less than 10^2. Therefore, the field penetration occurs anomalously fast. We can assume the presence of the effect of micro-instabilities or Hall processes. Micro-instabilities are accompanied with high-frequency magnetic-field oscillations. Stochastic noise in the low-hybrid frequency region is usually observed inside a rarefied laboratory mini-magnetosphere [30], but in our experiments it was absent during the passage of the laser-produced plasma. As for Hall processes, they manifest themselves when the Hall parameter – the ratio of the characteristic size to the ion plasma length – becomes approximately equal to or less than unity. For a laser-produced plasma density of ~10^{14} cm^{-3} and a magnetosphere size of ~25 cm, this parameter is ~10.

Another mechanism of magnetic field penetration into the plasma involves the development of groove instability at the plasma–magnetic field boundary. In Ref. [35], this mechanism, along with other ones, was comprehensively studied both experimentally and using three-dimensional magnetohydrodynamic numerical simulations. The dimensionless parameters of the present experiment and the experiment conducted in Ref. [35] are generally similar, despite the significantly different absolute values of the magnetic field, the interaction scale, the plasma density and temperature. The fundamental difference lies in the geometry of the interaction. In Ref. [35], the magnetic field is constant in space and the conical laser-produced plasma flow is rapidly transformed into a relatively thin sheet of thickness of the order of ion-plasma length. Under these conditions, the groove instability and Hall effects, in combination with the anomalous diffusion, enable the field to quickly penetrate the plasma. In our experiments, the pressure of the magnetic field rapidly decreased with distance, and the kinematic plasma pressure exceeded it in the entire domain under consideration. The structure of the plasma plume in the present experiment has larger dimensions than in the experiment of Ref. [35], and therefore the field cannot quickly penetrate the plasma.

Thus, the main conclusion of the work is that the effect of laser-produced plasma interaction with a magnetic field has been discovered, which is difficult to explain proceeding from the well-known and best-studied processes, and therefore additional experiments are called for.

Acknowledgements. This work was supported by the Russian Science Foundation (Grant No. 18-12-00080), the Russian Foundation for Basic Research (Grant Nos 18-29-21018 and 19-02-00993) and was carried out as part of the State Assignment of the Ministry of Science and Higher Education of the Russian Federation (Topic No. AAAA-A17-117021750017-0).

References

1. Keilhacker M., Kornherr M., Niedermeyer H., Steuer K.-H., Chodura R. *Proc. of the Fourth Int. Conf. on Plazma Physics and Controlled Nuclear Fusion Research* (Madison, USA, International Atomic Energy Agency, 1971) Vol. III, pp 265–276.
2. Cheung A.Y., Goforth R.R., Koopman D.W. *Phys. Rev. Lett*., **31** 429 (1973).
3. Borovsky J.E., Pongratz M.B., Roussel-Dupre R.A., Tan T.-H. *Astrophys. J.*, **280**, 802 (1973).
4. Antonov V.M., Bashurin V.P., Golubev A.I., Zhmailo V.A., Zakharov Yu.P., Orishich A.M., Ponomarenko A.G., Posukh V.G., Snytnikov V.N. *J. Appl. Mech. Tech. Phys*., **26**, 757 (1985).
5. Golubev A.I., Solov'ev A.A., Terekhin V.A. *J. Appl. Mech. Tech. Phys*., **19**, 602 (1978).
6. Winske D., Gary S.P. *J. Geophys. Res. A: Space Phys*., **112**, A10 (2007).
7. Longmire C.L. *Notes on Debris-Air Magnetic Interaction* (Santa Monica, Cal, Rand Corporation, Report RM-3386-PR, 1963).
8. Wright T.P. *Phys. Fluids*, **14**, 1905 (1971).
9. Zakharov Yu.P. et al. *Proc. VI Int. Symp. on Modern Problems of Laser Physics* (Novosibirsk, Russia, 2013) pp 193, 194.
10. Shaikhislamov I.F., Zakharov Yu.P., Posukh V.G., Melekhov A.V., Boyarintsev E.L., Ponomarenko A.G., Terekhin V.A. *Plasma Phys. Rep*., **41**, 399 (2015).
11. Podgornyi I.M., Sagdeev R.Z. *Sov. Phys. Usp*., **12**, 445 (1970) [*Usp. Fiz. Nauk*, **98**, 409 (1969)].
12. Baranov V.Yu. *Teplofiz. Vys. Temp*., **4** (5), 621 (1966).
13. Schindler K. *Space Sci. Rev*., **17**, 589 (1975).
14. Antonov V.M., Boyarintsev E.L., Zakharov Yu.P., Melekhov A.V., Posukh V.G., Ponomarenko A.G., Shaikhislamov I.F., in *Sovremennye dostizheniya v plazmennoi geliofizike* (Modern Advances in Plasma Heliophysics) (Moscow: 2018) pp 396–418.
15. Ponomarenko A.G., Zakharov Yu.P., Nakashima H., Antonov V.M., Melekhov A.V., Nikitin S.A., Posukh V.G., Shaikhislamov I.F., Muranaka T. *Adv. Space Res*., **28**, 1175 (2001).
16. Ponomarenko A.G., Antonov V.M., Posukh V.G., Melekhov A.V., Boyarintsev E.L., Afanasyev D.M., Yurkov R.N. *Report on MinPromNauka Project Investigation of Solar Activity and its Magnifications in Near Earth Space and Atmosphere. Part III* (Russia, 2004).
17. Ponomarenko A.G., Zakharov Yu.P., Antonov V.M., Boyarintsev E.L., Melekhov A.V., Posukh V.G., Shaikhislamov I.F., Vchivkov K.V. *Plasma Phys. Controlled Fusion*, **50**, 074015 (2008).
18. Zakharov Yu.P., Ponomarenko A.G., Antonov V.M., Boyarintsev E.L., Melekhov A.V., Posukh V.G., Shaikhislamov I.F. *IEEE Trans. Plasma Sci*., **35**, 813 (2007).
19. Zakharov Yu.P., Antonov V.M., Boyarintsev E.L., Melekhov A.V., Posukh V.G., Shaikhislamov I.F., Vchivkov K.V., Nakashima H., Ponomarenko A.G. *J. Phys.: Conf. Ser*., **112**, 042011 (2008).
20. Shaikhislamov I.F., Antonov V.M., Zakharov Yu.P, Boyarintsev E.L., Melekhov A.V., Posukh V.G., Ponomarenko A.G. *Plasma Phys. Controlled Fusion*, **51**, 105005 (2009).
21. Shaikhislamov I.F., Zakharov Y.P., Posukh V.G., Boyarintsev E.L., Melekhov A.V., Antonov V.M., Ponomarenko A.G. *Plasma Phys. Controlled Fusion*, **53**. 035017 (2011).
22. Shaikhislamov I.F., Zakharov Yu.P., Posukh V.G., Melekhov A.V., Antonov V.M., Boyarintsev E.L., Ponomarenko A.G. *Plasma Phys. Controlled Fusion*, **56**, 125007 (2014).
23. Halekas J.S., Mitchell D.L., Lin R.P., Hood L.L., Acuña M.H., Binder A.B. *Geophys. Res. Lett*., **29** (10), 77 (2002).
24. Shaikhislamov I.F., Antonov V.M., Zakharov Yu.P., Boyarintsev E.L., Melekhov A.V., Posukh V.G., Ponomarenko A.G. *Adv. Space Res*., **52**, 422 (2013).
25. Shaikhislamov I.F., Zakharov Yu.P., Posukh V.G., Melekhov A.V., Antonov V.M., Boyarintsev E.L., Ponomarenko A.G. *Plasma Phys. Controlled Fusion*, **56**, 025004 (2014).
26. Shaikhislamov I.F., Posukh V.G., Melekhov A.V., Zakharov Yu.P., Boyarintsev E.L., Ponomarenko A.G. *Plasma Phys. Controlled Fusion*, **57**, 075007 (2015).
27. Omidi N., Blanco-Cano X., Russell C.T., Karimabadi H., Acuna M. *J. Geophys. Res*., **107**, 1487 (2002).
28. Blanco-Cano X., Omidi N., Russell C.T. *J. Geophys. Res*., **108**, 1216 (2003).
29. Rumenskikh M.S., Chibranov A.A., Efimov M.A., Berezutskii A.G., Posukh V.G., Zakharov Yu.P., Boyarintsev E.L., Miroshnichenko I.B., Shaikhislamov I.F. *Pis'ma Zh. Eksp. Teor. Fiz*., **111** (6), 335 (2020).
30. Shaikhislamov I.F. et al. *Plasma Phys. Controlled Fusion*, **58** (11), 115002 (2016).
31. Khodachenko M.L., Alexeev I., Belenkaya E., Lammer H., Grießmeier M.J., Leitzinger M., Odert P., Zaqarashvili T., Rucker H.O. *Astrophys. J*. **744** (1),70 (2012).
32. Khodachenko M.L., Shaikhislamov I.F., Lammer H., Prokopov P.A. *Astrophys. J*., **813**, 50 (2015).
33. Antonov V.M., Boyarinsev E.L., Boyko A.A., Zakharov Y.P., Melekhov A.V., Ponomarenko A.G., Posukh V.G., Shaikhislamov I.F., Khodachenko M.L., Lammer H. *Astrophys. J*., **769**, 28 (2013).
34. Funaki I., Kimura T., Ueno K., et al. *Proc. 30th Int. Electric Propulsion Conf*. (Florence, IEPC-2007-94, 2007).
35. Khiar B., Revet G., Ciardi A., et al. *Phys. Rev. Lett*., **123**, 205001 (2019).